



Optics Letters

Loss-tolerant and quantum-enhanced interferometer by reversed squeezing processes

LONG TIAN,^{1,2,†} WENXIU YAO,^{1,†} YIMIAO WU,¹ QINGWEI WANG,¹ HENG SHEN,^{1,2}  YAOHUI ZHENG,^{1,2,*}  AND KUNCHI PENG^{1,2}

¹State Key Laboratory of Quantum Optics and Quantum Optics Devices, Institute of Opto-Electronics, Shanxi University, Taiyuan 030006, China

²Collaborative Innovation Center of Extreme Optics, Shanxi University, Taiyuan, Shanxi 030006, China

[†]These authors contributed equally to this work

*yhzheng@sxu.edu.cn

Received 8 February 2023; revised 28 June 2023; accepted 29 June 2023; posted 30 June 2023; published 20 July 2023

Reversed nonlinear dynamics is predicted to be capable of enhancing the quantum sensing in unprecedented ways. Here, we report the experimental demonstration of a loss-tolerant (external loss) and quantum-enhanced interferometer. Two cascaded optical parametric amplifiers are used to judiciously construct an interferometry with two orthogonal squeezing operation. As a consequence, a weak displacement introduced by a test cavity can be amplified for measurement, and the measured signal-to-noise ratio is better than that of both conventional photon shot-noise limited and squeezed-light assisted interferometers. We further confirm its superior loss-tolerant performance by varying the external losses and comparing with both conventional photon shot-noise limited and squeezed-light assisted configurations, illustrating the potential application in gravitational wave detection. © 2023 Optica Publishing Group

<https://doi.org/10.1364/OL.487355>

Quantum-enhanced metrology is the use of quantum resources such as squeezing or entanglement to yield higher statistical precision than purely classical approaches, consequently surpassing the classical bound of the standard quantum limit inherent in probes using a finite number of uncorrelated particles [1–5]. Very often, the precise measurement of physical quantities ranging from magnetic and electric fields [6], frequency [7] to displacement [8] are obtained by mapping to a phase shift that can be determined using interferometric techniques. In particular, optical interferometry plays an essential role in the testing of and search for fundamental laws of nature, including relativity and the connection between quantum and gravitational physics, as well as applications in fields as diverse as measurement of length [9] and velocity, sensors for rotation [10], acceleration, vibration, and searching for dark matter axion [11].

Remarkably, squeezed states of light were used to improve the sensitivity of a gravitational-wave observatory LIGO, VIRGO, and GEO600 projects [12–14]. Despite squeezing allowing for the improved measurement precision for one observable, the

sensitivity enhancement is intrinsically limited by the noise added during the detection, especially when it is comparable or larger than the squeezed noise. Reversed nonlinear dynamics such as squeezing operation, is very much believed to be associated with quantum-enhanced sensing, overcoming such a limitation. Actually, noiseless amplification of weak signal by two reversed squeezing interactions has been observed in spin systems [15], trapped-ion mechanical oscillator [8], and circuit quantum electrodynamics [16]. In optics, this approach was originally suggested by Caves [17] aiming to obtain a loss-tolerant and quantum-enhanced optical interferometry. A variety of the generalized versions were boosted [18–23]. For instance, the non-degenerated version, the so-called SU(1,1) interferometer [24–31], replaces the passive beam splitters in the Mach–Zehnder interferometer with parametric amplifiers, consequently improving signal-to-noise ratio (SNR). A degenerated version was also demonstrated, exploiting entangled photon pairs as a quantum resource, which is probabilistic and post-selective [32,33]. Further, a SU(2)-in-SU(1,1) nested interferometer was presented, addressing the problem of the signal strength limitation of the SU(1,1) interferometry [34]. However, the original design that is more exportable in a context of gravitational wave detection remains experimentally unexplored due to challenges in implementing cascaded and reversed squeezing interaction.

Here, we report an experimental demonstration of a loss-tolerant and Caves-type quantum-enhanced interferometer (CQEI) by two cascaded, reversed squeezing interactions. As an essential prerequisite to such a scenario, two cascaded optical parametric amplifiers (OPAs) are utilized to accomplish the squeezing interaction with opposite sign. The bright squeezed state generated by the first OPA is important to provide sub-shot noise sensitivity, while the second one allows us to reach robustness against detection noise and losses. Importantly, attributed to technical improvements in phase noise and system loss to reduce the degradation from decoherence, unitarity of nonlinear dynamics is promised in a relatively large range of squeezing strength. To highlight the flexibility of our approach, we emulate the loss-tolerant and quantum-enhanced measurement of weak signal in a realistic optical interferometry by introducing

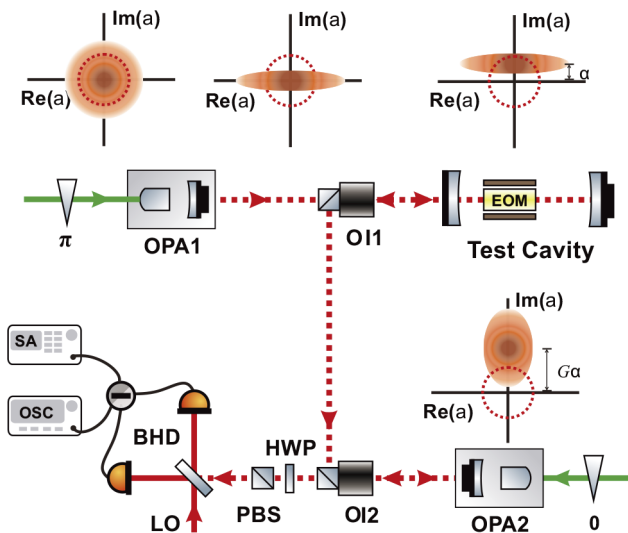


Fig. 1. Schematic diagram of loss-tolerant and quantum-enhanced interferometer by reversed squeezing processes: OPA, optical parametric amplifier; OI, optical isolator; EOM, electro-optical phase modulator; BHD, balanced homodyne detection; HWP, half-wave plate; PBS, polarization beam splitter; SA, spectrum analyzer; OSC, oscilloscope.

a test cavity. As the closest realization of the original Caves' proposal compatible with current LIGO and VIRGO detectors, it sheds light on the potential application in the gravitational wave detection.

Squeezing of optical fields here is implemented by an OPA, ideally depicted by the unitary operator $\hat{S}(\xi) = \exp[(\xi^* \hat{a}^2 - \xi \hat{a}^{\dagger 2})/2]$ with complex squeezing parameter $\xi = r \exp(i\theta)$. Here \hat{a} and \hat{a}^\dagger are, respectively, the annihilation and creation operators of the electromagnetic field, satisfying $[\hat{a}, \hat{a}^\dagger] = 1$. A conceptual architecture is illustrated in Fig. 1, and the protocol can be divided into three distinct sections. First, a squeezed state of light is generated by OPA1 with the interaction $\hat{S}(\xi_1)$ ($\xi_1 = r_1 e^{i\theta_1}$, $\theta_1 = \pi$) [35,36]. A small initial displacement α induced by the modulation from the test cavity is then applied along the squeezed axis to achieve the maximum amplification. This weak signal is finally amplified with ideal gain $G = e^{r_2}$ by the subsequent reversed squeezing $\hat{S}(\xi_2)$ from OPA2 with $\xi_2 = r_2 e^{i\theta_2}$ and $\theta_2 = 0$ [8]. A fascinating aspect of such a scheme is that, in stark contrast with the conventional protocol exploiting squeezing for enhanced metrology, building upon reversed configuration enables the detection loss-tolerant on the prerequisite of guaranteed sensitivity, surpassing the limit in the conventional interferometry (CI) and spectroscopy [28,37] (see Supplement 1 for more details).

To fully analyze the performance of such a CQEI, we consider the dissipation induced by the optical loss in the propagation. We sum up the loss that is caused by the non-unitary interaction of OPA1 and the propagation loss from OPA1 to the test cavity, and denote as $1 - T_1$, while $1 - T_2$ is introduced to describe the optical loss including the interaction loss with the test cavity and the propagation loss from the test cavity to OPA2. A weak displacement α along the \hat{p} -axis introduced by the test cavity in phase space. By summing up the dissipation in OPA2, the propagation loss and the total detection efficiency, we introduce the third effective transmission parameter T_3 . The associated

SNR_{CQEI} is (see Supplement 1 for more details)

$$\text{SNR}_{\text{CQEI}} = \frac{\sqrt{T_2 T_3} e^{r_2} \alpha}{\sqrt{T_3 T_2 T_1 e^{-2r_1} e^{2r_2} + T_3 (1 - T_1 T_2) e^{2r_2} + 1 - T_3}}. \quad (1)$$

A squeezed-light assisted interferometer (SAI) can be constructed by manipulating OPA2 to far detuning and block the pump beam of OPA2, giving the corresponding SNR_{SAI} as

$$\text{SNR}_{\text{SAI}} = \frac{\sqrt{T_2 T_3} \alpha}{\sqrt{T_3 T_2 T_1 e^{-2r_1} + 1 - T_1 T_2 T_3}}. \quad (2)$$

Here $1 - T_2$ arises from the interaction loss with the test cavity only.

We can easily conclude the SNR_{CI} for CI, i.e., photon shot-noise limited case,

$$\text{SNR}_{\text{CI}} = \sqrt{T_2 T_3} \alpha. \quad (3)$$

Our experimental demonstration uses two cascaded OPAs at 1064 nm to operate the squeezing of optical fields, where for each the semi-monolithic single resonant standing wave cavity is formed by a piezo-actuated concave mirror and the back surface of a periodically poled KTiOPO_4 crystal with a dimension of $1 \text{ mm} \times 2 \text{ mm} \times 10 \text{ mm}$ [38,39]. By means of balanced homodyne detection [40], we characterize both OPAs separately via measuring the pump power dependence of anti-squeezed and squeezed quadrature variances, exhibited in Fig. S4 (see Supplement 1 for more details).

A key requirement for implementing the reversed protocol should be satisfied: the orthogonality of two cascaded squeezing interaction. It is guaranteed by a Pound–Drever–Hall phase-locking technique with high precision. Specifically, OPA1 operates at amplification status by locking the relative phase between pump field and seed light to 0, while at OPA2 the relative phase between the pump field and the injected signal field from OPA1 is locked to π , that is to enforce the strict anti-squeezing interaction with respect to OPA1, i.e., realizing $\hat{S}(-\xi_2)$.

To demonstrate the loss-tolerant and quantum-enhanced measurement of a weak displacement, we use a 6.12 MHz-linewidth test cavity with a temperature-controlled electro-optical phase modulator (EOPM) inside [41,42] to generate a signal frequency of 12 MHz larger than the test cavity linewidth. This is what happens in a Michelson interferometer working close to the dark fringe, where the output quadrature is displaced by an amount given by the product between the arms phase difference and the coherent field amplitude. By doing so one can proof-of-principle emulate the quantum-enhanced sensing of a weak signal in a realistic optical interferometry, and the associated equivalence is demonstrated in Supplement 1. Here, in order to emulate the scheme of signal sensing in gravitational wave detection, the signal amplitude on the phase quadrature of squeezed light beam from OPA1, is tuned by locking the cavity length to different values, which affects the detuning of signal with respect to the resonance position of test cavity [43,44].

Figure 2 illustrates the measured SNR of our CQEI as a function of the squeezed degree of OPA2 given -7 dB bright squeezed state of light generated in OPA1 ($r_1 = 0.8$). Thanks to the noise suppression, injecting squeezed light into the interferometer [gray dash line in Fig. 2(a)] improves the SNR with respect to the conventional shot-noise limited configuration [gray solid line in Fig. 2(a)]. By introducing the second reversed

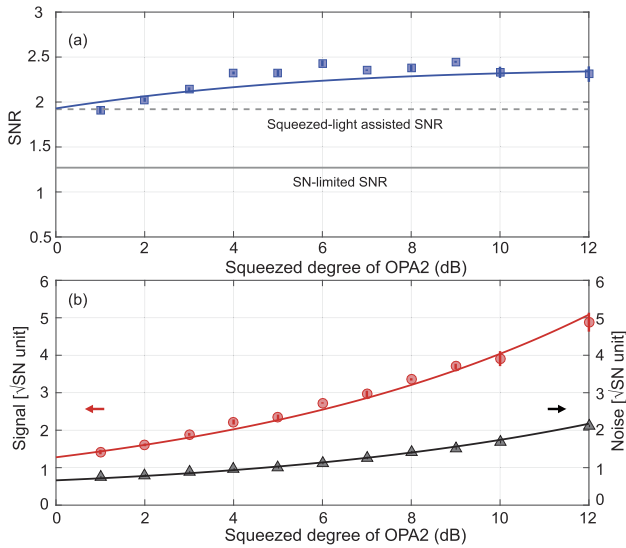


Fig. 2. (a), (b) Measured SNR and signal or noise level of the CQEI as a function of the squeezed degree of OPA2. In (a), blue squares display the experimental values with $T_1 = 0.92$, $T_2 = 0.90$, $T_3 = 0.85$, $\alpha = 1.45$, $r_1 = 0.8$, while the blue solid line gives the theoretical results by taking into account of the dissipation. Gray dashed line shows the SNR of the SAI, and the gray solid line is the CI SNR, shot noise-limited SNR. Measured signal and noise level as a function of the squeezed degree of OPA2 in (b), with the values shown in a linear format. The black triangle and red circles display the experimental noise and signal values, respectively. The black and red solid line show the theoretical results by taking into account of the dissipation. Each data point is measured at the analysis frequency of 12 MHz.

squeezing interaction, weak displacement signal is amplified considerably while the noise is not deteriorated significantly, as shown in Fig. 2(b). In consequence, the SNR of our protocol [blue square in Fig. 2(a)] is better than other two configurations, agreeing with the theoretical model [blue solid line in Fig. 2(a)] accounting for optical losses and phase locking uncertainty (see Supplement 1 for more details).

We proceed to characterize the loss-tolerant performance of the CQEI by comparing with other two protocols aforementioned. The loss-tolerant mechanism of the demonstrated quantum interferometer is outlined in the reconstructed Wigner function distribution in phase space [45] shown in Figs. 3(a)–3(c). Figure 3(a) depicts the conventional shot-noise limited case ($\text{SNR}_{CI} = 1.27$, $T_1 = 0.92$, $T_2 = 0.90$, $T_3 = 0.85$). The squeezed-light assisted configuration is realized as follows. We first generate a -7 dB-squeezed state of light in \hat{p} -quadrature with OPA1 [$\hat{q} = (\hat{a} + \hat{a}^\dagger)/\sqrt{2}$ and $\hat{p} = (\hat{a} - \hat{a}^\dagger)/i\sqrt{2}$], followed by a small displacement $\alpha = 1.45$ along squeezed axis- \hat{p} [Fig. 3(b)]. Due to the optical loss that is caused by the optical isolator, the final detected phase noise level was only -3.6 dB, so that $\text{SNR}_{SAI} = 1.27/\sqrt{10^{-0.1 \times 3.6}} = 1.92$. Moreover, by additionally reversing the squeezing interaction with OPA2 ($r_2 = 1.15$), the optical fields return to the amplitude-squeezed state with a magnified amplitude $G\alpha = 3.356$ and the phase noise level of 3 dB [Fig. 3(c)]. We can calculate that $\text{SNR}_{CQEI} = 3.356/\sqrt{10^{0.1 \times 3}} = 2.376$. Worthy of attention is that the optimal SNR is not always obtained for the same working point, it depends on the squeezed degree of the OPA and losses. The

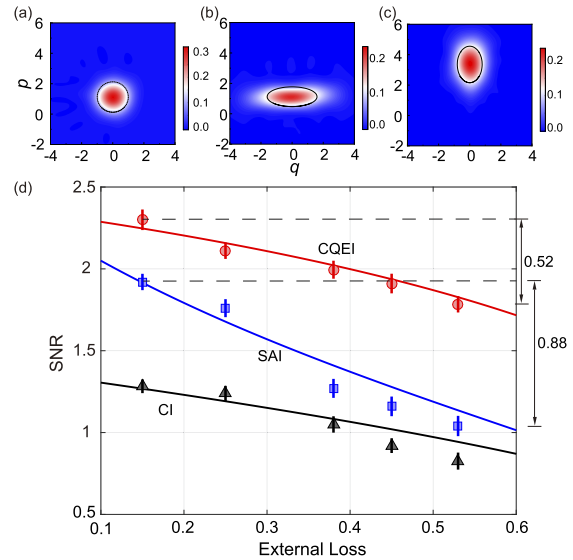


Fig. 3. Experimental results of quantum-enhanced-interferometer of a displacement $\alpha = 1.45$ with -7 dB squeezing operation. (a)–(c) Reconstructed Wigner functions distribution in phase space are obtained via the iterative maximum-likelihood estimation. The black lines in the figure represent the noise contours of the reconstructed Wigner function distribution at half maximum (a) for the CI; (b) for the SAI; (c) for the CQEI. (d) Measured SNR as the function of the external loss. The black triangle, blue square, and red circle display the SNR of the CI, SAI, and CQEI, respectively. Solid lines indicate the corresponding theoretical values.

CQEI is much more immune to the noise adding during the detection (including non-perfect quantum efficiency and optical losses) than that in squeezed-light assisted scheme. This is confirmed by varying the external loss, i.e., by tuning the angle of the half-wave plate before the final balanced homodyne detection, as presented in Fig. 3(d) (see Supplement 1 for more details). When the external loss increases from 0.15 to 0.53, the decrease of SNR is 0.88 for SAI, and 0.52 for CEQI. It is seen that the SNR of the SAI is more fragile to the dissipation associated with the external loss than other two cases, and, furthermore, our approach shows the best SNR.

We have presented a new architecture of a loss-tolerant and quantum-enhanced interferometer, the closest version to the original design for gravitational wave detection [17]. Our results merge the rich physics of reversed nonlinear dynamics and their ability for high sensitivity quantum sensing with the unique properties of time reversible interferometry. In contrast to conventional squeezing-enhanced quantum metrology it is more robust to detection loss. Our methods are also applicable to the microwave domain [11, 16, 46]. Compared with a non-degenerate SU(1, 1) interferometer [24, 28], our protocol is compatible with current gravitational wave detection such as LIGO and VIRGO detectors [13, 17, 47–51], and further, is immune to any unequal perturbations suffered by the two arms, which degrades the performance of such a non-degenerate SU(1, 1) interferometer. Most important, our protocol is universal and independent on the baseline wavelength. The proposed baseline wavelength of the next gravitational wave detector is in the mid-infrared region, to make use of the low coating absorption and reduced optical loss and scatter properties of silicon, in order to improve on

thermal and scatter noise. But subject to the current fabrication technology, the maximum quantum efficiency of the photodiode is limited, resulting in the extra noise added due to imperfect detection. Yet, our approach can reduce the requirement on the quantum efficiency of the corresponding photodiode.

Funding. National Natural Science Foundation of China (62225504, 62027821, U22A6003, 62035015, 12174234, 12274275); National Key Research and Development Program of China (2020YFC2200402); Key Research and Development Program of Shanxi (202102150101003); Program for Sanjin Scholar of Shanxi Province.

Disclosures. The authors declare no conflicts of interest.

Data availability. Data underlying the results presented in this paper are not publicly available at this time but may be obtained from the authors upon reasonable request.

Supplemental document. See Supplement 1 for supporting content.

REFERENCES

- V. Giovannetti, S. Lloyd, and L. Maccone, *Nat. Photonics* **5**, 222 (2011).
- V. Giovannetti, S. Lloyd, and L. Maccone, *Science* **306**, 1330 (2004).
- C. L. Degen, F. Reinhard, and P. Cappellaro, *Rev. Mod. Phys.* **89**, 035002 (2017).
- N. Treps, U. Andersen, B. Bucher, P. K. Lam, A. Maître, H. A. Bachor, and C. Fabre, *Phys. Rev. Lett.* **88**, 203601 (2002).
- Y. Q. Ma, H. X. Miao, B. H. Pang, M. Evans, C. N. Zhao, J. Harms, R. Schnabel, and Y. Chen, *Nat. Photonics* **13**, 776 (2017).
- J. F. Barry, J. M. Schloss, E. Bauch, M. J. Turner, C. A. Hart, L. M. Pham, and R. L. Walsworth, *Rev. Mod. Phys.* **92**, 015004 (2020).
- Boulder Atomic Clock Optical Network (BACON) Collaboration, *Nature* **591**, 564 (2021).
- S. C. Burd, R. Srinivas, J. J. Bollinger, A. C. Wilson, D. J. Wineland, D. Leibfried, D. H. Slichter, and D. T. C. Allcock, *Science* **364**, 1163 (2019).
- H. Stiebig, V. Mandryka, E. Bunte, H. J. Büchner, and K. Jun, *J. Non-Cryst. Solids* **338-340**, 793 (2004).
- M. P. Hokmabadi, A. Schumer, D. N. Christodoulides, and M. Khajavikhan, *Nature* **576**, 70 (2019).
- K. M. Backes, D. A. Palken, and S. A. Kenany, *et al.*, *Nature* **590**, 238 (2021).
- H. Grote, K. Danzmann, K. L. Dooley, R. Schnabel, J. Slutsky, and H. Vahlbruch, *Phys. Rev. Lett.* **110**, 181101 (2013).
- J. Aasi, J. Abadie, and B. P. Abbott, *et al.*, *Nat. Photonics* **7**, 613 (2013).
- F. Acernese, M. Agathos, and L. Aiello, *et al.*, *Phys. Rev. Lett.* **123**, 231108 (2019).
- D. Linnemann, H. Strobel, W. Muessel, J. Schulz, R. J. Lewis-Swan, K. V. Kheruntsyan, and M. K. Oberthaler, *Phys. Rev. Lett.* **117**, 013001 (2016).
- M. Malnou, D. A. Palken, B. M. Brubaker, L. R. Vale, G. C. Hilton, and K. W. Lehnert, *Phys. Rev. X* **9**, 021023 (2019).
- C. M. Caves, *Phys. Rev. D* **23**, 1693 (1981).
- X. J. Zuo, Z. H. Yan, Y. N. Feng, J. X. Ma, X. J. Jia, C. D. Xie, and K. C. Peng, *Phys. Rev. Lett.* **124**, 173602 (2020).
- G. F. Jiao, K. Y. Zhang, L. Q. Chen, C. H. Yuan, and W. P. Zhang, *Photonics Res.* **10**, 475 (2022).
- W. Du, J. F. Chen, Z. Y. Ou, and W. P. Zhang, *Appl. Phys. Lett.* **117**, 024003 (2020).
- Y. H. Liu, J. M. Li, L. Cui, N. Huo, S. M. Assad, X. Y. Li, and Z. Y. Ou, *Opt. Express* **26**, 27705 (2018).
- A. Ferreri, M. Santandrea, M. Stefszky, K. H. Luo, H. Herrmann, C. Silberhorn, and P. R. Sharapova, *Quantum* **5**, 461 (2021).
- E. Giese, S. Lemieux, M. Manceau, R. Fickler, and R. W. Boyd, *Phys. Rev. A* **96**, 053863 (2017).
- Z. Y. Ou, *Phys. Rev. A* **85**, 023815 (2012).
- A. M. Marino, N. V. C. Trejo, and P. D. Lett, *Phys. Rev. A* **86**, 023844 (2012).
- B. E. Anderson, P. Gupta, B. L. Schmittberger, T. Horrom, C. Hermann-Avigliano, K. M. Jones, and P. D. Lett, *Optica* **4**, 752 (2017).
- Y. Michael, L. Bello, M. Rosenbluh, and A. Péér, *npj Quantum Inf.* **5**, 81 (2019).
- Z. Y. Ou and X. Y. Li, *APL Photonics* **5**, 080902 (2020).
- M. Manceau, F. Khalili, and M. Chekhova, *New J. Phys.* **19**, 013014 (2017).
- A. A. Clerk, M. H. Devoret, S. M. Girvin, F. Marquardt, and R. J. Schoelkopf, *Rev. Mod. Phys.* **82**, 1155 (2010).
- C. M. Caves, *Adv. Quantum Technol.* **3**, 1900138 (2020).
- G. Frascella, S. Agne, F. Y. Khalili, and M. V. Chekhova, *npj Quantum Inf.* **7**, 72 (2021).
- M. Manceau, G. Leuchs, F. Khalili, and M. Chekhova, *Phys. Rev. Lett.* **119**, 223604 (2017).
- W. Du, J. Kong, G. Z. Bao, P. Y. Yang, and J. Jia, *Phys. Rev. Lett.* **128**, 033601 (2022).
- U. L. Andersen, T. Gehring, C. Marquardt, and G. Leuchs, *Phys. Scr.* **91**, 053001 (2016).
- K. McKenzie, N. Grosse, W. P. Bowen, S. E. Whitcomb, M. B. Gray, D. E. McClelland, and P. K. Lam, *Phys. Rev. Lett.* **93**, 161105 (2004).
- B. Yurke, S. L. McCall, and J. R. Klauder, *Phys. Rev. A* **33**, 4033 (1986).
- W. H. Yang, S. P. Shi, Y. J. Wang, W. G. Ma, Y. H. Zheng, and K. C. Peng, *Opt. Lett.* **42**, 4553 (2017).
- S. P. Shi, L. Tian, Y. J. Wang, Y. H. Zheng, C. D. Xie, and K. C. Peng, *Phys. Rev. Lett.* **125**, 070502 (2020).
- X. L. Jin, J. Su, Y. H. Zheng, C. Y. Chen, W. Z. Wang, and K. C. Peng, *Opt. Express* **23**, 23859 (2015).
- Z. X. Li, W. G. Ma, W. H. Yang, Y. J. Wang, and Y. H. Zheng, *Opt. Lett.* **41**, 3331 (2016).
- M. R. Huo, J. L. Qin, J. L. Cheng, Z. H. Yan, Z. Z. Qin, X. L. Su, X. J. Jia, C. D. Xie, and K. C. Peng, *Sci. Adv.* **4**, eaas9401 (2018).
- J. Südbeck, S. Steinlechner, M. Korobko, and R. Schnabel, *Nat. Photonics* **14**, 240 (2020).
- M. J. Yap, P. Altin, T. G. McRae, B. J. J. Slagmolen, R. L. Ward, and D. E. McClelland, *Nat. Photonics* **14**, 223 (2020).
- A. I. Lvovsky and M. G. Raymer, *Rev. Mod. Phys.* **81**, 299 (2009).
- A. Eddins, S. Schreppler, D. M. Toyli, L. S. Martin, S. Hacohe-Gourgy, L. C. G. Govia, H. Ribeiro, A. A. Clerk, and I. Siddiqi, *Phys. Rev. Lett.* **120**, 040505 (2018).
- R. S. Bondurant and J. H. Shapiro, *Phys. Rev. D* **30**, 2548 (1984).
- Y. Zhao, N. Aritomi, and E. Capocasa, *et al.*, *Phys. Rev. Lett.* **124**, 171101 (2020).
- L. McCuller, C. Whittle, and D. Ganapathy, *et al.*, *Phys. Rev. Lett.* **124**, 171102 (2020).
- A. Abramovici, W. E. Althouse, and R. W. P. Drever, *et al.*, *Science* **256**, 325 (1992).
- H. Yu, L. McCuller, M. Tse, N. Kijbunchoo, L. Barsotti, and N. Mavalvala, members of the LIGO Scientific Collaboration, *Nature* **583**, 43 (2020).